The Life Cycle of the Northern Hemisphere Sudden Stratospheric Warmings

Varavut Limpasuvan

Department of Chemistry and Physics, Coastal Carolina University, Conway, South Carolina

David W. J. Thompson

Department of Atmospheric Science, Colorado State University, Fort Collins, Colorado

Dennis L. Hartmann

Department of Atmospheric Sciences, University of Washington, Seattle, Washington

ABSTRACT

Motivated by recent evidence of strong stratospheric–tropospheric coupling during the Northern Hemisphere winter, this study examines the evolution of the atmospheric flow and wave fluxes at levels throughout the stratosphere and troposphere during the composite life cycle of a sudden stratospheric warming. The composite comprises 39 major and minor warming events using 44 years of NCEP–NCAR reanalysis data. The incipient stage of the life cycle is characterized by preconditioning of the stratospheric zonal flow and anomalous, quasi-stationary wavenumber-1 forcing in both the stratosphere and troposphere. As the life cycle intensifies, planetary wave driving gives rise to weakening of the stratospheric polar vortex and downward propagation of the attendant easterly wind and positive temperature anomalies. When these anomalies reach the tropopause, the life cycle is marked by momentum flux and mean meridional circulation anomalies at tropospheric levels that are consistent with the negative phase of the Northern Hemisphere annular mode. The anomalous momentum fluxes are largest over the Atlantic half of the hemisphere and are associated primarily with waves of wavenumber 3 and higher.

1. Introduction

Sudden stratospheric warmings (SSWs) dominate the variability of the Northern Hemisphere (NH) wintertime stratospheric circulation (e.g., see Andrews et al. 1987). During a SSW, polar stratospheric temperatures rise and the zonal-mean zonal flow weakens dramatically over a short time period. As the zonal flow weakens, the stratospheric circulation becomes highly asymmetric and the stratospheric polar vortex is displaced off the pole. In the most dramatic cases, stratospheric temperatures can rise by ~50°C and the stratospheric circumpolar flow can reverse direction in the span of just a few days.

Sudden stratospheric warmings involve interactions between the zonal flow of the polar stratosphere and upward propagating planetary waves consisting primarily of zonal wavenumbers 1 and 2 (e.g., Matsuno 1971; Andrews et al. 1987). When a vertically propagating wave enters the polar stratosphere, it imparts a

westward acceleration there through wave dissipation or wave transience. The deceleration of the eastward zonal flow is offset by the Coriolis force acting on an induced poleward residual circulation that flows across the axis of the eddy forcing. By continuity, the anomalous poleward residual circulation requires sinking (rising) motion below and poleward (equatorward) of the forcing region. The adiabatic temperature changes associated with these induced residual meridional motions act to weaken the meridional temperature gradient, as required by thermal wind balance, and give rise to the warming observed in the polar stratosphere.

The presence of vertically propagating waves is a necessary, but not sufficient condition for a SSW to occur; the stratospheric zonal flow must also be "preconditioned" such that wave activity is focused toward the polar vortex (e.g., Labitzke 1981; Butchart et al. 1982; McIntyre 1982). The polar vortex is generally preconditioned when the zonal flow is displaced poleward such that it appears "tighter" about the pole. In this case, the relatively small mass and moment of inertia of the vortex allow upward-propagating waves to exert considerable influence on the circulation through wave forcing (McIntyre 1982). The preconditioning of the vortex is typically initiated by a precursor planetary

Corresponding author address: Dr. Varavut Limpasuvan, Department of Chemistry and Physics, Coastal Carolina University, P.O. Box 261954, Conway, SC 29528.
E-mail: var@coastal.edu

wave that breaks along the periphery of the vortex (Dunkerton et al. 1981). However, the preconditioning of the vortex may also be a function of low frequency vacillations in the stratospheric circulation in which anomalies in the stratospheric zonal flow are drawn poleward and downward on time scales of several months (e.g., Holton and Mass 1976; Kodera et al. 2000; Kodera and Kuroda 2000; Kuroda 2002).

Sudden stratospheric warmings have been historically viewed as a stratospheric phenomenon, but increasing evidence shows that they may also have a marked influence on the circulation of the troposphere. Anecdotal evidence of the impact of SSWs on the circulation of the troposphere was first presented in Quiroz (1977), who observed large temperature changes in the troposphere in association with the sudden stratospheric, warming event of 1976/77 (see also O'Neill and Taylor 1979). Recently, Baldwin and Dunkerton (1999) examined 40 years of daily data and found that large amplitude anomalies in the lower-stratospheric zonal flow typically descend throughout the depth of the stratosphere on a time scale of weeks and that the largest amplitude anomalies in the stratosphere frequently appear to descend to tropospheric levels. Baldwin and Dunkerton (2001) subsequently found that the surface signature of these downward propagating anomalies strongly resembles the surface signature of the Northern Hemisphere annular mode (NAM), a large-scale pattern of climate variability associated with out-of-phase fluctuations of the zonal flow between centers of action located near 35° and 55° latitude (e.g., Hurrell 1995; Thompson and Wallace 1998, 2000). Zhou et al. (2002) observed similar downward propagation in stratospheric temperatures.

In support of these observations, numerous modeling experiments have demonstrated a distinct tropospheric response to circulation anomalies imposed at polar stratospheric levels (e.g., O'Neill 1980; O'Neill et al. 1982; Boville 1984; Polvani and Kushner 2002; Norton 2003; Taguchi 2003), and several theories have been proposed in an effort to explain how variability in the stratosphere can impact the circulation of the troposphere. One theory involves the impact of the stratospheric circulation on the index of refraction of vertically propagating waves (e.g., Chen and Robinson 1992; Hartmann et al. 2000; Shindell et al. 2001). At a given level, the index of refraction for vertically propagating planetary waves is a function of the strength of the zonal flow (e.g., Chen and Robinson 1992; Hu and Tung 2002; Lorenz and Hartmann 2003). When the zonal flow is very strong in the lower polar stratosphere, vertically propagating waves tend to be deflected equatorward, and vice versa. Since the eddy flux of westerly momentum is in the opposite direction of the wave propagation, it follows that regions below levels of strong zonal flow (and hence anomalous vertical shear) will be marked by anomalous convergence of zonal momentum by waves, and vice versa. Hence, while wave energy ultimately originates at tropospheric levels, the above mechanism will tend to draw large amplitude anomalies in the zonal flow of the stratosphere downward with time. It also provides a possible mechanism whereby large amplitude zonal wind anomalies at lower stratospheric levels can impact the circulation of the upper troposphere.

Another mechanism whereby the anomalous stratospheric circulation can impact the troposphere can be interpreted as a variant on the dynamics of "downward control" (Haynes et al. 1991). In the context of downward control, momentum forcing at stratospheric levels is transported to the surface via an induced meridional circulation. Since the stratosphere contains at most about 25% of the total mass of the extratropical atmosphere during the winter season, this mechanism is generally dismissed as incapable of driving anomalies in the tropospheric circulation. Nevertheless, recent evidence suggests that downward control can drive comparatively large anomalies in the troposphere if the stratospheric anomalies project onto the preferred modes of variability of the tropospheric circulation such as the NAM (Black 2002; Robinson 2004). Another variant of the so-called downward control principal was proposed by Ambaum and Hoskins (2002). In this case, potential vorticity (PV) anomalies in the lower stratosphere lead to deformations in the height of the polar tropopause that, in turn, give rise to similarly signed PV anomalies at tropospheric levels.

The purpose of this study is to provide a comprehensive analysis of the atmosphere at levels throughout the troposphere and stratosphere during SSWs. In contrast to Baldwin and Dunkerton (1999, 2001), we analyze results, not only for the zonal flow, but also for the fluxes of momentum and heat by eddies of varying spatial and temporal scales and for the mean meridional circulation. By fully documenting the evolution of various dynamical quantities during observed SSWs, the results provide a benchmark for assessing numerical simulations of the influence of SSWs on the circulation of the troposphere and provide a physical reference for theories that seek to explain the observed linkages between stratospheric and tropospheric variability. As discussed below, our key findings demonstrate that both quasi-stationary planetary waves and smaller-scale transients maintain the tropospheric wind anomalies against surface friction as the stratospheric warming matures. The rest of the paper is divided into three sections: The methodology and data are discussed in section 2, the results are presented in section 3, and section 4 offers a synthesis of the principal findings of the study.

2. Data and analysis

This study uses 44 years of data (1958–2001) from the National Centers for Environmental Prediction–National Center for Atmospheric Research (NCEP–NCAR) reanalysis project (Kalnay et al. 1996). The dataset con-
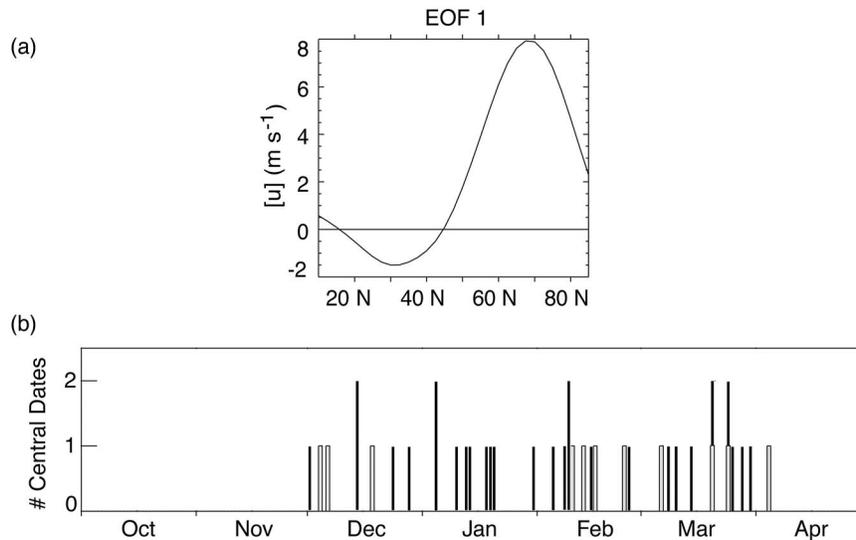
FIG. 1. (a) The leading EOF structure of the zonal-mean zonal wind anomalies, [**u**], at 50 hPa shown as a regression map between the corresponding leading PC (i.e., the SZI) and the wind anomalies. (b) The occurrence of the 39 central dates. From left to right, the year corresponding to each bar is *1958,* 1996, *1981,* 1965 and *1987,* 2000, *1968,* 1998, 1998 and 1994, 1977, *1968, 1960,* 1985, 1970, *1971,* 1995, *1973, 1987,* 1991 and 1992, *1968,* 1963, *1960, 1958, 1973,* 1966, *1981,* 1999, 1984, 1989, *1971* and 1980, 1983 and 1961, 1964, 1975, 1974, and 1978. The years in italic font indicate the presence of more than one central date. Black bars (28 in all) indicate events that correspond to sudden stratospheric major warmings (26) and minor warmings (2) as defined by the WMO.
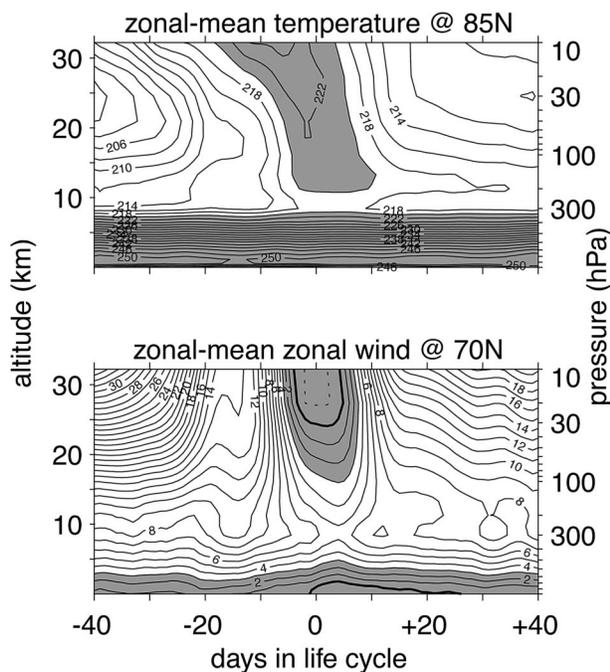

FIG. 2. (top) Total zonal-mean temperature at 85°N and (bottom) zonal-mean zonal wind at 70°N during the composite life cycle of SSWs. Temperature warmer than 220 K is shaded. Wind amplitude less than 3 m s⁻¹ is shaded.

tains daily averages of geopotential height, wind, and temperature on a $2.5° \times 2.5°$ grid at 17 vertical pressure levels extending from 1000 to 10 hPa. All anomalies presented in this study are computed as departures from the daily climatological annual cycle determined from the entire 44-yr record.

Variability in the strength of the stratospheric polar vortex is defined on the basis of the leading principal component (PC) time series of daily zonal-mean zonal wind anomalies at 50 hPa during the extended winter season (October–April). When forming the temporal covariance matrix for the PC, the grid points in the horizontal data domain were weighted by the square root of the cosine of latitude. Hereafter referred to as the stratospheric zonal index (SZI), the resulting first PC time series (associated with the first empirical orthogonal function mode) explains about 54% of the total variance in the 50-hPa zonal-mean wind field and is well separated from the subsequent (higher) modes based on the criterion of North et al. (1982). The pattern found by regressing zonal-mean zonal wind anomalies at 50 hPa onto the standardized SZI describes out-of-phase fluctuations in the stratospheric zonal-mean flow with a node centered near 45°N (Fig. 1a). By definition, positive values of the SZI correspond to stronger than normal westerlies poleward of 45°N. The results presented below are fairly insensitive to the stratospheric level chosen as the basis of the SZI. For example, similar results are derived for the SZI defined at 10 hPa; how-
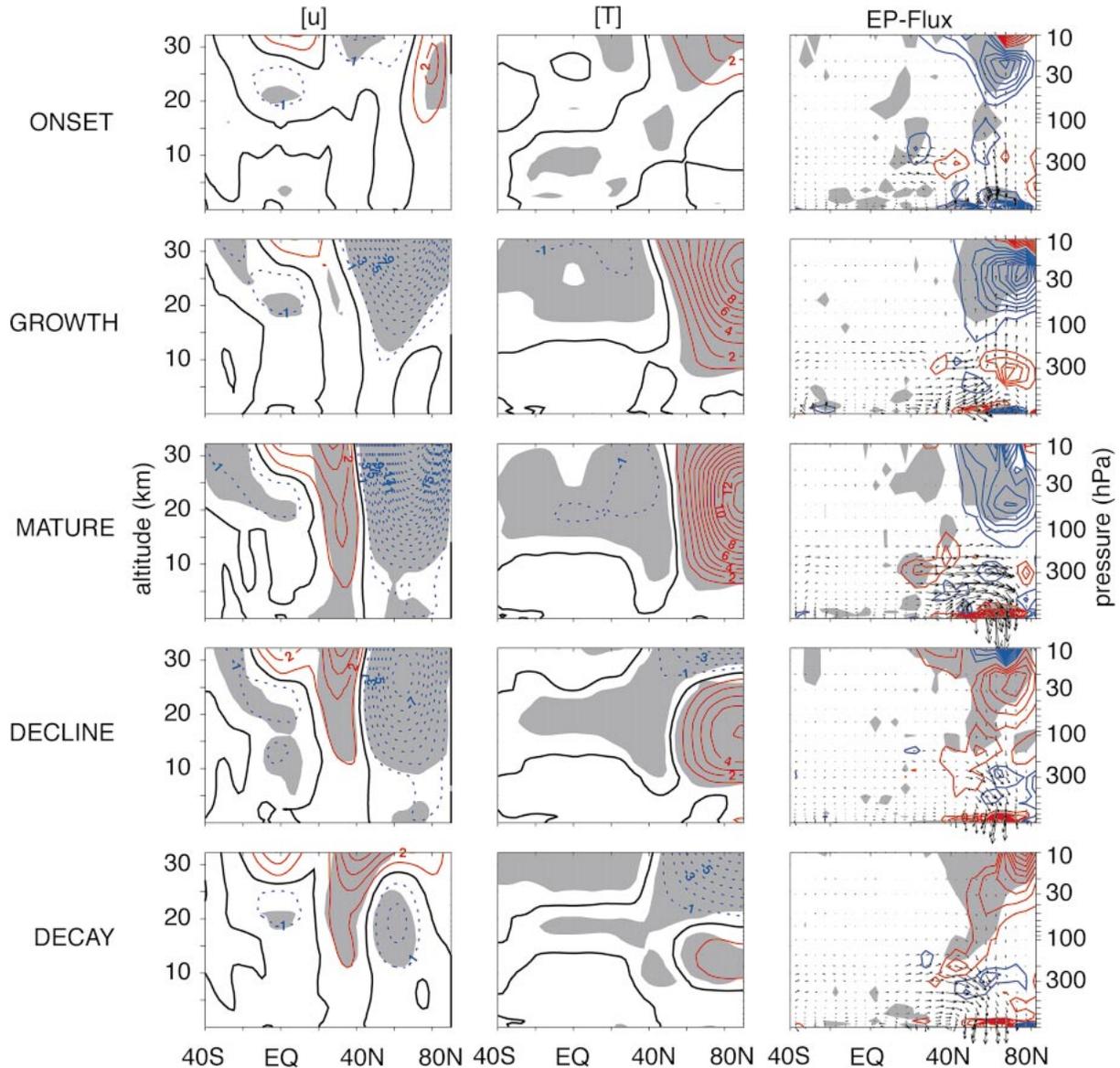
FIG. 3. (left) Anomalous zonal-mean zonal wind, (middle) zonal-mean temperature, and (right) EP flux with its divergence during the composite life cycle of SSWs. Negative contours are given as blue dashes. Zero contours are given as bold solid lines. The wind (temperature) contour interval is 1 m s^{-1} (1 K). The EP flux divergence (divided by $\rho_o a \cos\theta$, where ρ_o is basic density, a is the earth's radius, and θ is latitude) is contoured in the right column at every 0.25 m s^{-1} day^{-1} with deceleration in blue. The vector lengths in the right column are referenced with respect to the top figure in the column. Gray shading indicates areas with a 95% confidence level (based on t statistics).

ever, the leading PC/EOF at 10 hPa is not separated from the higher modes.

The occurrence of a SSW is determined by the amplitude of the 15-day low-pass SZI. Weakenings of the vortex commence when the low-pass SZI drops below one standard deviation below its long-term mean. The central date of a weakening (referred to as day 0) is the midpoint between the day when the SZI drops below −1 standard deviation and when it rises again above −1 standard deviation. The central date corresponds closely to the time when the polar westerlies are at their

weakest (see Fig. 2). Each SSW event is taken to be 81 days in duration (40 days before and after day 0).

Overall, 39 SSW events were chosen based on the above criteria. The central dates associated with these events occur between early December and early April and exhibit a weak bias toward more events during late winter (Fig. 1b). A representative *life cycle* of these SSWs is defined as the composite average of the 39 events. In the results below, we present the life cycle by dividing it into five 15-day increments that reflect the *onset* (days −37 to −23), *growth* (days −22 to −8),
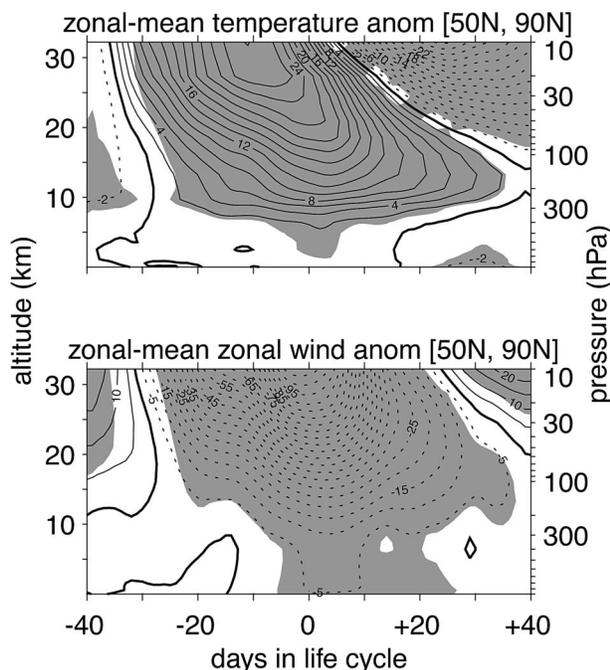
FIG. 4. Zonal-mean temperature anomalies and zonal-mean zonal wind anomalies integrated poleward of 50°N during the composite life cycle of SSWs. Negative contours are given as dashes. Zero contours are given as a bold solid line. Contour interval for temperature (zonal wind) is 2 K (5 m s⁻¹). Dark gray shading indicates areas with a 95% confidence level (based on *t* statistics).

maturation (days −7 to +7), *decline* (days +8 to +22), and *decay* (days +24 to +37) of a typical sudden stratospheric warming. Here, the negative (positive) times indicate days prior to (after) the central date (or day 0). Additionally, we present the life cycle as altitude–time sections of latitudinally integrated variables for the entire 81-day period.

By construction, the selected events coincide closely to sudden stratospheric warmings as defined by the World Meteorological Organization (WMO; see the black vertical bars in Fig. 1b). According to the WMO definition, a stratospheric warming occurs when the latitudinal gradient in 10-hPa zonal-mean temperatures between 85° and 60°N is positive for more than 5 days. If the 10-hPa zonal-mean zonal wind at 65°N is concurrently easterly, the warming event is categorized as a ''major warming''; otherwise, the warming event is categorized as ''minor'' (see Andrews et al. 1987). A total of 26 of the 39 events used in this study correspond to WMO-defined major warmings and 2 of the events correspond to WMO-defined minor warmings. The remaining 11 events correspond to weakenings of the polar vortex that are neither WMO-defined major nor minor warmings.

As shown in Fig. 2, the *total* zonal-mean temperature at 85°N and zonal-mean zonal wind at 70°N of the composite life cycle describe the rapid polar warming and weakening of the stratospheric zonal flow consistent

with the evolution of major sudden warmings described in previous case studies (e.g., Andrews et al. 1987; Kodera and Chiba 1995). The rapid breakdown of the stratospheric zonal flow is preceded by a period of relatively cold conditions and strong circumpolar flow and is followed by the gradual recovery of the stratospheric polar vortex. Thus, while the mature stage of the composite sudden stratospheric warming lasts only a few weeks, it is embedded in a cycle of lower frequency variability consisting of the preconditioning of the stratospheric zonal flow and the slow recovery of the polar vortex.

3. The life cycle of a sudden stratospheric warming

Figure 3 shows the composite of the anomalous zonal-mean zonal wind, zonal-mean temperature, and the Eliassen–Palm (EP) flux during the life cycle of sudden stratospheric warmings. During the onset stage, the zonal flow in the extratropical stratosphere is anomalously weak equatorward of 60°N, but anomalously strong poleward of 70°N. Hence, the vortex is anomalously constricted about the pole and appears preconditioned for effective wave forcing (McIntyre 1982; Andrews et al. 1987). At this time, the stratosphere is disturbed by marked heat flux anomalies above 100 hPa in connection with vertically propagating waves along the node of the anomalous wind anomalies (~60°N). The attendant convergence of the EP flux in the stratosphere gives rise to significant anomalous easterly forcing poleward of 50°N above 100 hPa. Significant but weak warm temperature anomalies are found over the pole above 30 hPa. The relatively weak easterly anomalies centered near 50 hPa at the equator found throughout the composite life cycle are the hallmark of the easterly phase of the equatorial quasi-biennial oscillation (QBO), which favors an increased frequency of occurrence of SSWs (Holton and Tan 1980).

During the onset, growth, and mature stages of the composite SSW, the convergence of the EP flux, the weakening of the zonal flow, and the warming of the polar cap all descend from the middle to lower stratosphere. By the mature stage, the amplitudes of the zonal wind and temperature anomalies peak in the stratosphere, and easterlies are observed from the surface to the top of the analysis. At this time, the warming of the polar stratosphere is peaked near 50 hPa. The anomalous wave fluxes in the troposphere are directed poleward from ~40°–70°N near 300 hPa and downward along 60°N.

Starting in the mature phase, the anomalous stratospheric wave flux is downward, which implies anomalously low planetary wave activity as the vortex recovers. In the decline stage, both the wind and temperature anomalies in the stratosphere weaken and descend in altitude. During the decay stage, the easterly wind anomalies have nearly disappeared (although still
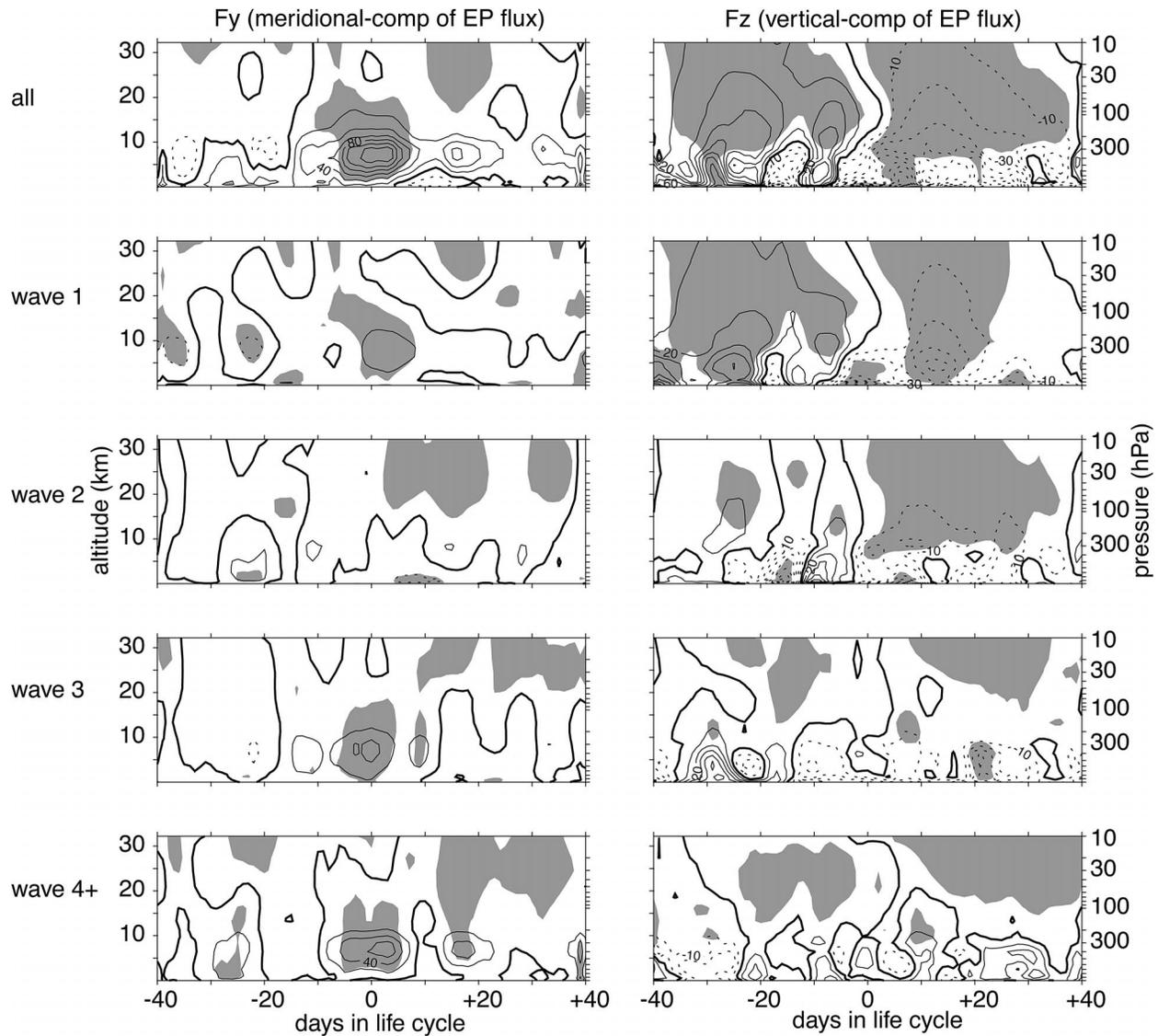
FIG. 5. Vertical and horizontal component of anomalous EP flux integrated poleward of 50°N for all and various wavenumbers during the composite life cycle of SSWs. Contribution from combined wavenumbers greater than or equal to 4 is denoted by "wave 4+." The sum of "wave 1," "wave 2," "wave 3," and "wave 4+" produces the result for "all." Contours of the vertical component and horizontal component are given every 10×10^4 kg s^{-2} and 20×10^6 kg s^{-2}, respectively. Negative contours are given as dashes. Zero contours are given as a bold solid line. Dark gray shading indicates areas with a 95% confidence level (based on t statistics).

significant), and the significant warm temperature anomalies have descended to 200 hPa.

The poleward and downward movement of the anomalous zonal-mean wind and temperature from the upper stratosphere to the lower stratosphere throughout the life cycle of the composite SSW is reminiscent of the stratospheric vacillation cycles observed by Kodera et al. (2000), Kodera and Kuroda (2000), and Kuroda (2002). The coincidence of downward propagation in the zonal flow with downward propagation of the EP-flux convergence suggests that the vacillation cycle is driven by wave–mean flow interactions in the stratosphere. The cold temperature anomalies in the polar stratosphere

above 30 hPa in the decay stage suggest the onset of a vacillation cycle of opposite sign, though the time scale of a typical SSW generally accounts for a substantial fraction of the winter season.

The largest amplitudes in Fig. 3 are found at stratospheric levels, but substantial anomalies are also observed at tropospheric levels. Consistent with the results presented in Baldwin and Dunkerton (1999, 2001), weakenings of the stratospheric zonal flow descend not only throughout the stratosphere, but into the troposphere as well. The most striking tropospheric features in Fig. 3 are the pronounced EP fluxes in the troposphere during the mature phase of the event. At this time, the
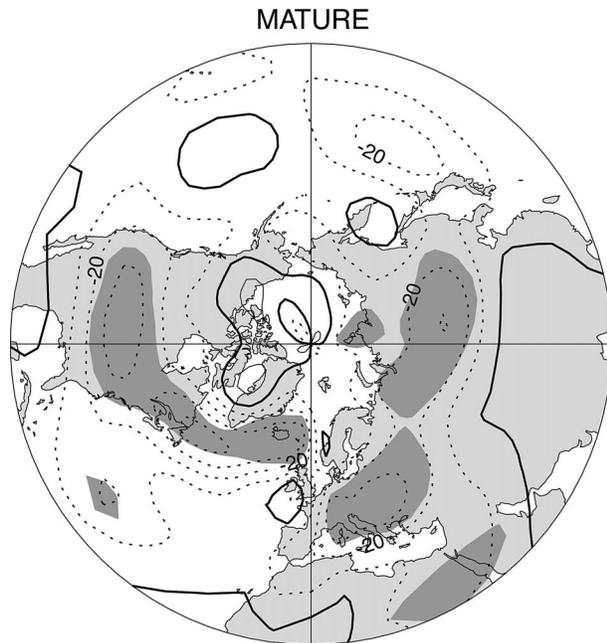
MATURE

FIG. 6. Time-averaged distribution of u^*v^* anomalies during the mature phase (time average between day −7 and day +7) of SSWs. Here, the asterisk denotes a departure from zonal symmetry. The variables u and v are zonal wind and meridional wind, respectively. Negative values are given as dashes and represent anomalous equatorward momentum fluxes. Dark gray shading indicates areas with a 95% confidence level (based on t statistics).

upper-tropospheric circulation is marked by both anomalous equatorward momentum fluxes above 500 hPa and by anomalously weak poleward heat fluxes in the lower troposphere. Hence the composite suggests that enhanced eddy momentum fluxes near the tropopause play a key role in transmitting the stratospheric anomalies to tropospheric levels.

The vertically varying temporal evolution of the composite SSW is explored further in Figs. 4–7. As shown in Fig. 4, the zonal-mean temperature and zonal wind anomalies over the polar region (integrated from 50° to 90°N) propagate downward in a manner consistent with that observed in Baldwin and Dunkerton (1999, 2001). At 10 hPa, the maximum warm anomalies precede the easterly wind anomalies by about 10 days. Significant easterly wind anomalies appear near the surface around day 0 where they persist thereafter for about 10 days.

During both the weakening and recovery of the stratospheric zonal flow, the stratospheric heat flux anomalies are almost entirely associated with zonal wavenumber-1 disturbances (Fig. 5, right). In contrast, the pronounced upper-tropospheric momentum flux anomalies that peak during the mature phase are associated primarily with waves of wavenumber 3 and higher (Fig. 5, left). The anomalous momentum fluxes are largest over the North Atlantic half of the hemisphere, which suggests that weakenings of the stratospheric polar vortex project particularly strongly onto variations in the North Atlantic

storm track and jet stream (Fig. 6). Zhou et al. (2002) report a similar bias toward the North Atlantic sector in their observations of changes in the upper-tropospheric circulation following stratospheric temperature anomalies.

While the eddy momentum fluxes due to zonal wavenumbers less than 3 in Fig. 5 are presumably associated with planetary waves, the physical nature of the "wave 4+" eddy fluxes is less clear. This is explored further in Fig. 7, which shows the temporal decomposition of the eddy fluxes into contributions by quasi-stationary time scales (>40 days), synoptic time scales (<15 days), and residual time scales (defined here as time scales between 15 and 40 days and the attendant interactions with the quasi-stationary and synoptic time scales). The formulation and definition of the time-filtering technique follows directly from Lorenz and Hartmann (2003). Note that the combined sum of the time-filtered eddy flux components ("all" in Fig. 7) is identical to the independently computed, combined sum of the spatially filtered eddy flux components ("all" in Fig. 5).

As expected, the anomalous heat fluxes in the stratosphere associated primarily with wavenumbers 1 and 2 (Fig. 5) are dominated by quasi-stationary time scales (Fig. 7). However, the anomalous momentum fluxes in the upper troposphere associated primarily with wavenumbers 3 and higher (Fig. 5) are attributable not only to quasi-stationary time scales, but also to synoptic and residual time scales. It is interesting that the synoptic time scale eddies also make a significant contribution to the equatorward heat flux (negative **Fz**) around day 0.

The residual zonal-mean meridional circulation (Fig. 8, left) is directed poleward between 10 and 50 hPa from days ~−30 to 0 and equatorward at the surface starting around day 0. The NCEP–NCAR data has no vertical wind observations above ~18 km, but the residual vertical wind in the upper troposphere implies residual sinking motion (and associated adiabatic warming) in the polar stratosphere prior to day 0. In the polar stratosphere, the anomalous Eulerian mean meridional circulation (Fig. 8a, right) is in the opposite sense of the residual circulation (consistent with the strong eddy heat fluxes there). In the troposphere, the anomalous Eulerian mean meridional circulation is associated with thermally indirect overturning motion consistent with a modulation of the Ferrell cell (Limpasuvan and Hartmann 1999; Thompson and Wallace 2000). Poleward of ~50°N, the anomalous tropospheric overturning cell is characterized by poleward motion in the upper troposphere, sinking motion over the polar cap, and equatorward motion at the surface (see boxed regions in Fig. 8). Between 10° and 50°N (Fig. 8b), the mature phase of the SSW is predominantly accompanied by equatorward motion in the upper troposphere, rising motion in the middle troposphere, and poleward motion near the surface.

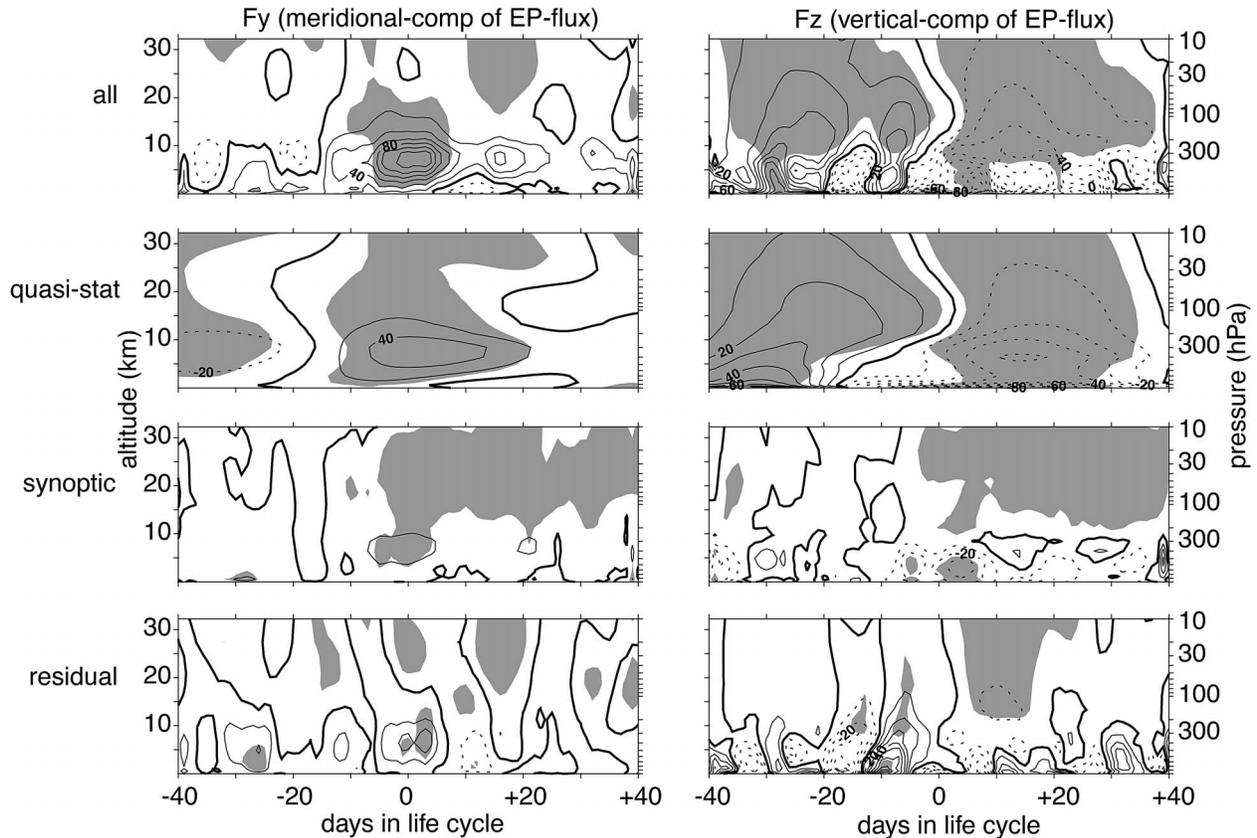The growth of the tropospheric overturning cell, re-

FIG. 7. Vertical and horizontal component of anomalous EP flux integrated poleward of 50°N for all and various time-filtered eddies during the composite life cycle of SSWs. The quasi-stationary, synoptic, and residual eddy momentum and heat fluxes (used to calculate the EP flux) are based on the methodology of Lorenz and Hartmann (2003). The sum of "quasi-stat," "synoptic," and "residual" produces the result for "all," which is identical to that shown in Fig. 5. Contour intervals, style, and shading are the same as in Fig. 5.

vealed in Fig. 8, coincides with the growth of the largest upper-tropospheric meridional EP flux (Figs. 5 and 7, left). Since the Coriolis force acting on the upper-tropospheric poleward flow acts to oppose the easterly anomalies there, it follows that the tropospheric overturning cell must be driven by the anomalous convergence of the eddy momentum flux. The Coriolis force acting on the equatorward (poleward) surface wind anomalies helps maintain the lower-tropospheric easterly (westerly) anomalies against frictional dissipation (see Fig. 3, [**u**]).

Figure 9 shows the composite SSW life cycle of the zonal varying, anomalous geopotential height field at 1000, 250, and 50 hPa. In the stratosphere, the significant wavenumber-1 disturbance evident during the onset stage in Fig. 5 is associated with an anomalous anticyclone over the Aleutian Islands and an anomalous cyclone over Russia (Fig. 9, top left column). At this time, significant wavenumber-1 anomalies are also evident near the surface, but with anomalously low heights over the North American half of the hemisphere and anomalously high heights over the Eurasian half of the hemisphere. The surface wavenumber-1 anomalies are also evident at 250 hPa, but are rotated westward with

height, consistent with the enhanced upward EP flux at this time (Figs. 3 and 5).

As the warming intensifies, the height anomalies are dominated by a high degree of zonal symmetry with anomalously high geopotential heights over the polar region and anomalously low geopotential heights throughout middle latitudes in both the stratosphere and troposphere. Consistent with Baldwin and Dunkerton (2001), the tropospheric anomalies during the mature phase bear a striking resemblance to the surface signature of the NAM. As the vortex recovers, the anomalous high-stratospheric heights are displaced off the pole while the NAM-like anomalies persist at the surface.

4. Summary

This study presents the atmospheric flow and the eddy fluxes of heat and momentum during the composite life cycle of a sudden stratospheric warming. The analysis incorporates both major and minor stratospheric warmings and makes no a priori distinction on the differing ways in which the vortex can be initially perturbed [e.g., Schoeberl (1978) notes that weaker warmings are gen-
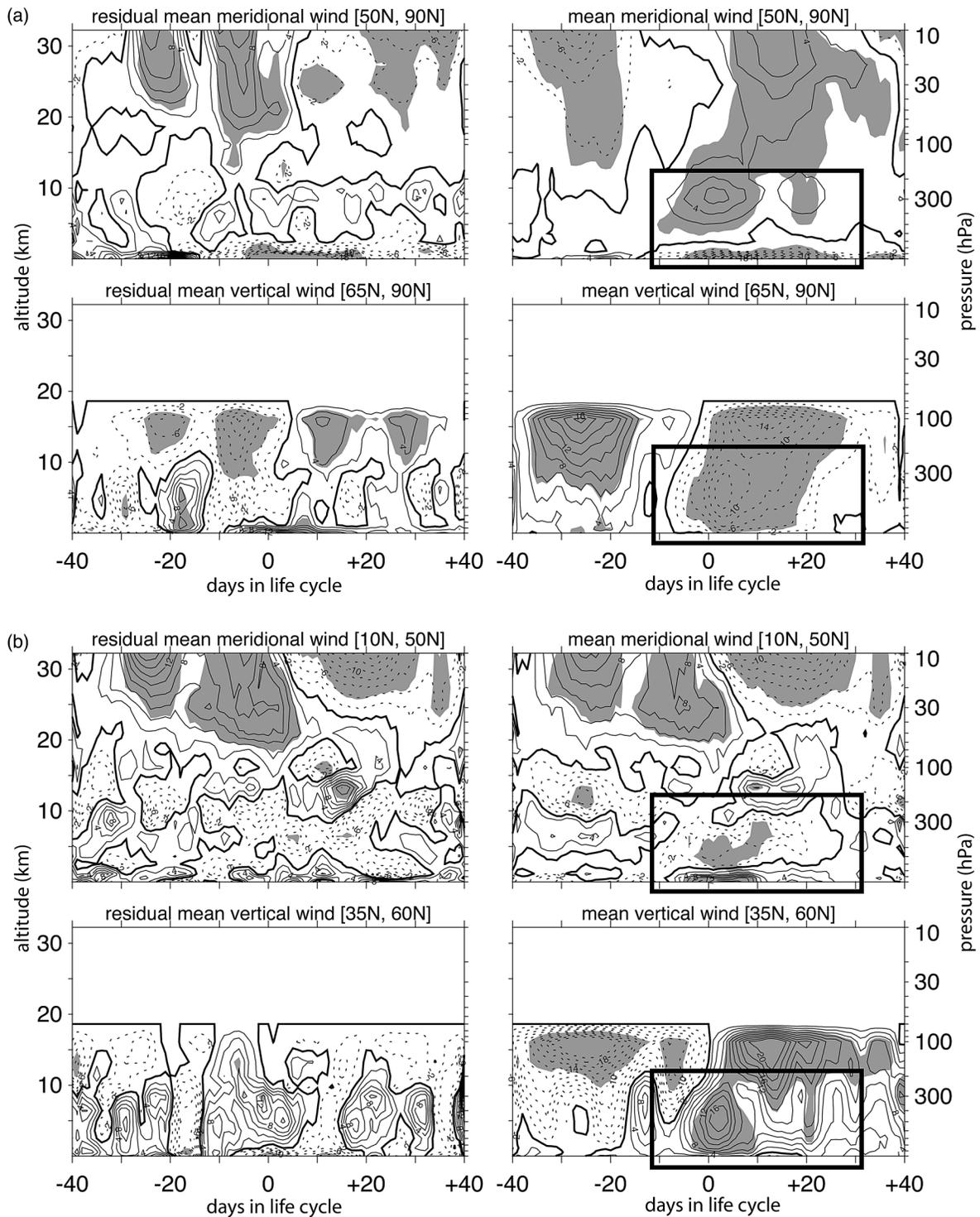
FIG. 8. (left) Residual zonal-mean circulation and (right) zonal-mean circulation during the composite life cycle of SSWs. (a) The meridional wind is integrated poleward of 50°N and its contour interval is 2 dam s⁻¹. Poleward motion is positive. The vertical wind is integrated poleward of 65°N and its contour interval is 2 × 10⁻¹ mm s⁻¹. Downward motion is negative. Note that the NCEP–NCAR data have no vertical wind observations above 18 km. Dark gray shading indicates areas with a 95% confidence level (based on *t* statistics). (b) As in (a) except that the integration is performed from 10°–50°N for meridional wind and 35°–60°N for vertical wind.
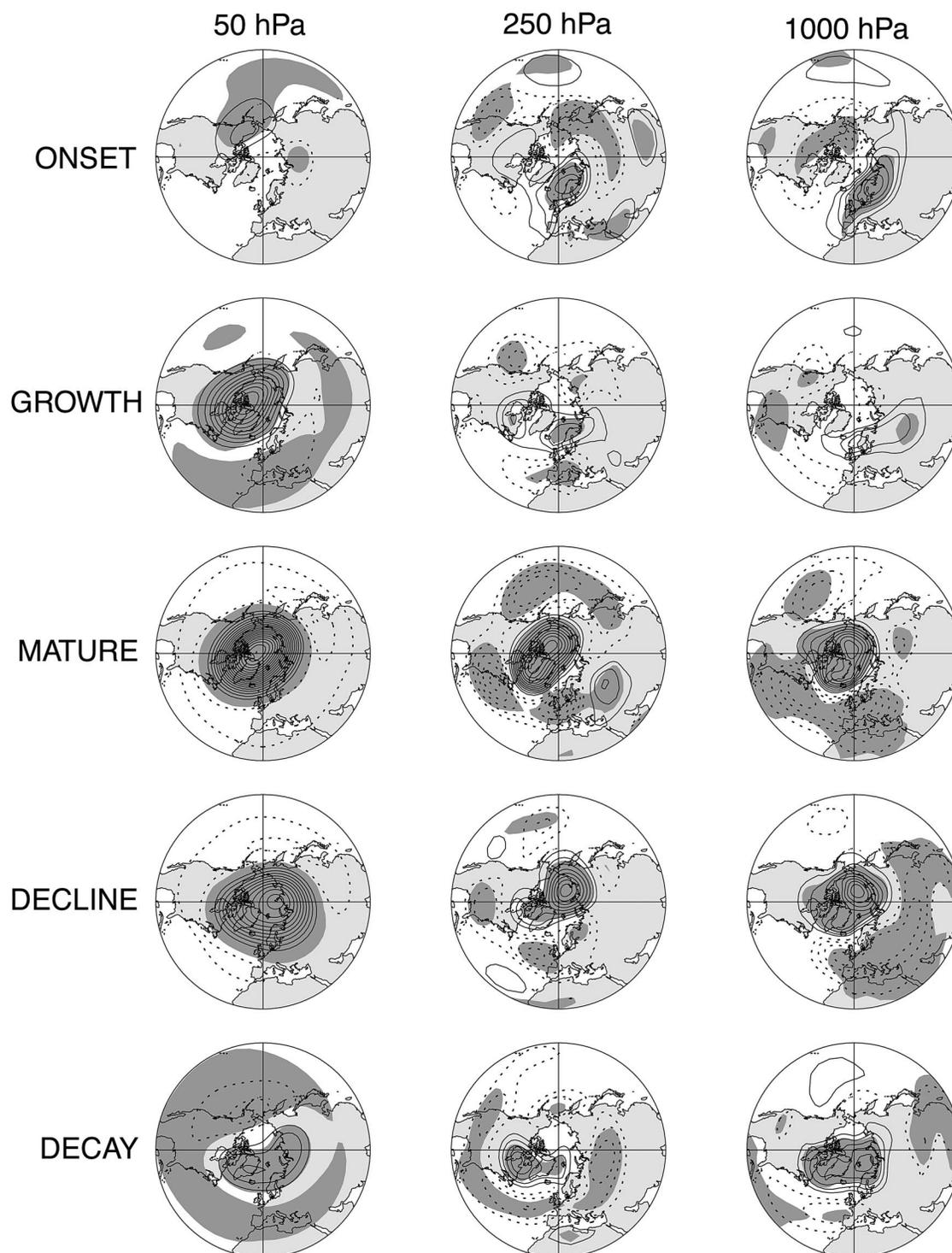
FIG. 9. Geopotential height anomalies [in decameters (dam)] at various levels during the composite life cycle of SSWs. The contour interval is 3, 1, and 0.5 dam for 50, 250, and 1000 hPa, respectively. Negative anomalies are shown as dashes. Zero contours are omitted for clarity. Dark gray shading indicates areas with 95% confidence level (based on *t* statistics).
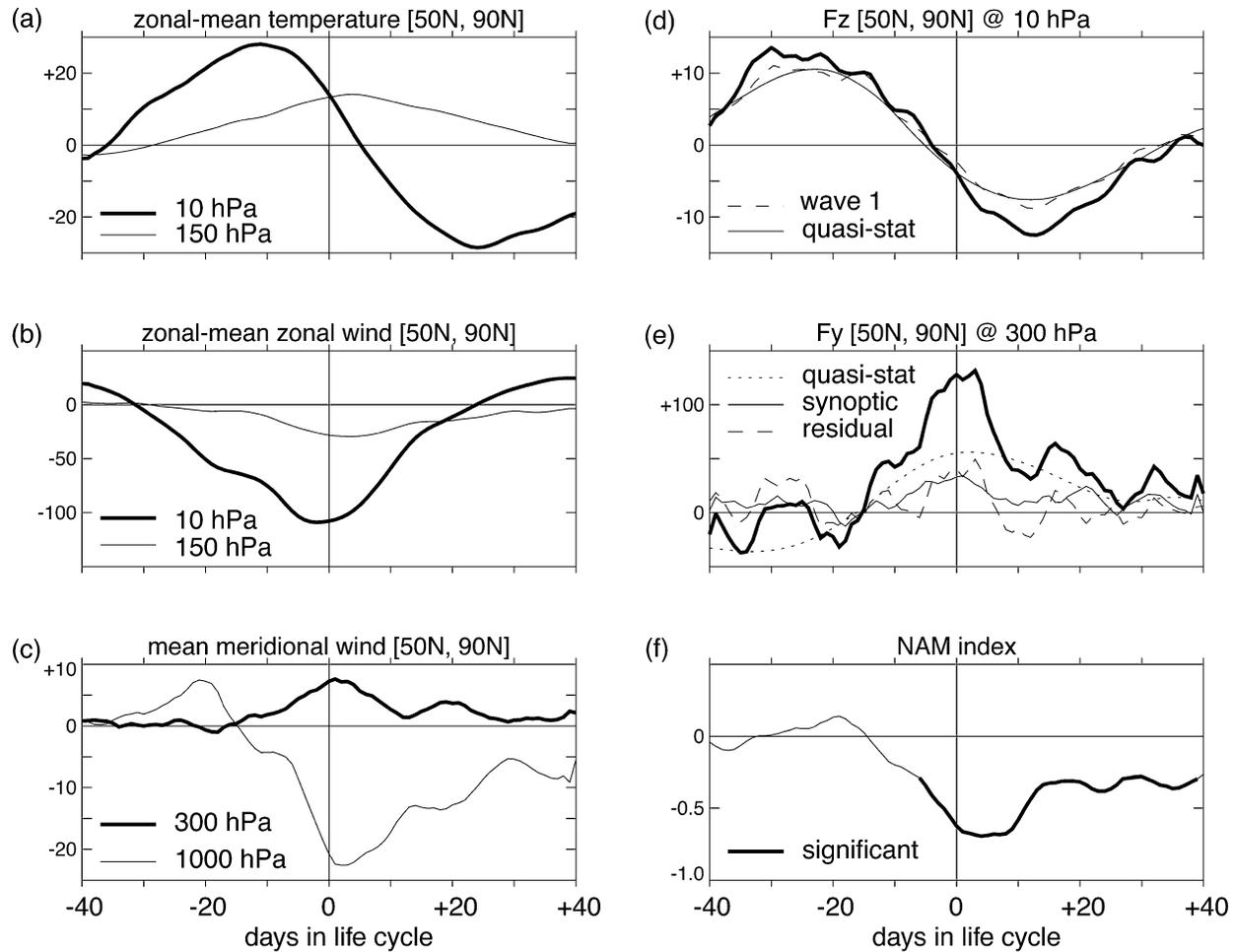
FIG. 10. (a)–(e) Various quantities integrated poleward of 50°N during the composite life cycle of SSWs. (f) The daily surface NAM index during the composite life cycle (the bold portion indicates the 95% confidence level).

erally associated with zonal wavenumber-2 disturbances; Yoden et al. (1999)]. The key results associated with the composite life cycle are summarized in Fig. 10.

Strong heat flux anomalies are observed in the preconditioned upper stratosphere several weeks before the weakest state of the polar vortex (Figs. 10a,b,d). The heat fluxes are associated mainly with quasi-stationary wavenumber-1 disturbances that are evident at both tropospheric and stratospheric levels. The intensification of anomalous poleward heat fluxes is followed by poleward motion in the stratospheric residual mean meridional circulation, easterly anomalies in the stratosphere centered at ~65°N, and strong warming of the polar stratosphere that descends in time as subsequent wave activity breaks at successively lower stratospheric levels (Figs. 3 and 10a,b). When the zonal wind anomalies reach the lower stratosphere (~150 hPa), strong equatorward momentum fluxes appear near 300 hPa (Fig. 10e) and strong equatorward heat flux anomalies appear in the lower troposphere (Fig. 3). The tropospheric momentum forcing precedes anomalies in the NAM by a

few days and is associated primarily with eddies of length scales smaller than wavenumber 3 (Fig. 5) that act on both quasi-stationary and transient time scales (Figs. 7 and 10e). The upper-tropospheric momentum flux anomalies are largest over the North Atlantic sector (Fig. 6). Also at this time, significant (Eulerian) mean meridional poleward motion develops near 300 hPa and equatorward motion develops at the surface (Figs. 8 and 10c).

The Coriolis force acting on the upper-tropospheric mean meridional wind anomalies in Fig. 10c opposes the anomalous convergence of the eddy momentum flux in middle latitudes, implied by Fig. 10e. The Coriolis torque acting on the surface branch of the meridional circulation anomalies drives easterly anomalies along ~55°–60°N and the corresponding meridional circulation anomalies equatorward of 40°N (Fig. 8b, right) give rise to near-surface westerly wind anomalies along ~30°N. Hence, the tropospheric features evident in Fig. 3 and the attendant negative bias in the NAM during the mature phase of the weakening (Fig. 10f; see also

Baldwin and Dunkerton 2001) can be interpreted as the response to the anomalous momentum fluxes. It is notable that the negative bias in the NAM lasts considerably longer than the associated momentum fluxes at 300 hPa.

The key results in this study are thus the following:

1) The downward propagating events in the stratospheric zonal flow associated with sudden stratospheric warmings (and as outlined in Baldwin and Dunkerton 1999, 2001) are preceded by preconditioning of the stratospheric circulation and by anomalous wavenumber-1 forcing in both the stratosphere and troposphere.
2) The downward-propagating anomalies in the stratospheric zonal flow are accompanied by downward propagating anomalies in the convergence of the EP flux, which suggests that this behavior reflects wave–mean flow interactions in the stratospheric circulation.
3) When the downward propagating wind anomalies reach the tropopause level, the tropospheric circulation is marked by large anomalies in the flux of heat and momentum by waves smaller than wavenumber 3. The results suggest that the key dynamical processes that underlie the observed coupling between the stratospheric and tropospheric circulations lie in the linkage between variability in the zonal flow of the lower stratosphere and wave activity in the troposphere.

REFERENCES

Ambaum, M. H. P., and B. J. Hoskins, 2002: The NAO troposphere–stratosphere connection. *J. Climate,* **15,** 1969–1978.

Andrews, D. G., J. R. Holton, and C. B. Leovy, 1987: *Middle Atmospheric Dynamics.* Academic Press, 489 pp.

Baldwin, M. P., and T. J. Dunkerton, 1999: Propagation of the Arctic Oscillation from the stratosphere to the troposphere. *J. Geophys. Res.,* **104,** 30 937–30 946.

——, and ——, 2001: Stratospheric harbingers of anomalous weather regimes. *Science,* **294,** 581–584.

Black, R. X., 2002: Stratospheric forcing of surface climate in the Arctic Oscillation. *J. Climate,* **15,** 268–277.

Boville, B. A., 1984: The influence of the polar night jet on the tropospheric circulation in a GCM. *J. Atmos. Sci.,* **41,** 1132–1142.

Butchart, N., S. A. Clough, T. N. Palmer, and P. J. Trevelyan, 1982: Simulations of an observed stratospheric warming with quasi-geostrophic refractive index as a model diagnostic. *Quart. J. Roy. Meteor. Soc.,* **108,** 475–502.

Chen, P., and W. A. Robinson, 1992: Propagation of planetary waves between the troposphere and stratosphere. *J. Atmos. Sci.,* **49,** 2533–2545.

Dunkerton, T. J., C.-P. F. Hsu, and M. E. McIntyre, 1981: Some Eulerian and Lagrangian diagnostics for a model stratospheric warming. *J. Atmos. Sci.,* **38,** 819–843.

Hartmann, D. L., J. M. Wallace, V. Limpasuvan, D. W. J. Thompson, and J. R. Holton, 2000: Can ozone depletion and global warming interact to produce rapid climate change? *Proc. Natl. Acad. Sci. USA,* **97,** 1412–1417.

Haynes, P. H., C. J. Marks, M. E. McIntyre, T. G. Shepherd, and K. P. Shine, 1991: On the ''downward control'' of extratropical diabatic circulations by eddy-induced mean zonal forces. *J. Atmos. Sci.,* **48,** 651–679.

Holton, J. R., and C. Mass, 1976: Stratospheric vacillation cycles. *J. Atmos. Sci.,* **33,** 2218–2225.

——, and H.-C. Tan, 1980: The influence of the equatorial quasi-biennial oscillation on the global circulation at 50 mb. *J. Atmos. Sci.,* **37,** 2200–2208.

Hu, Y., and K. K. Tung, 2002: Interannual and decadal variations of planetary-wave activity, stratospheric cooling, and Northern Hemisphere annular mode. *J. Climate,* **15,** 1659–1673.

Hurrell, J. W., 1995: Decadal trends in the North Atlantic Oscillation: Regional temperatures and precipitation. *Science,* **269,** 676–679.

Kalnay, E., and Coauthors, 1996: The NCEP/NCAR 40-Year Reanalysis Project. *Bull. Amer. Meteor. Soc.,* **77,** 437–471.

Kodera, K., and M. Chiba, 1995: Tropospheric circulation changes associated with stratospheric sudden warmings: A case study. *J. Geophys. Res.,* **100,** 11 055–11 068.

——, and Y. Kuroda, 2000: A mechanistic model study of slowly propagating coupled stratosphere–troposphere variability. *J. Geophys. Res.,* **105,** 12 361–12 370.

——, ——, and S. Pawson, 2000: Stratospheric sudden warmings and slowly propagating zonal-mean zonal wind anomalies. *J. Geophys. Res.,* **105,** 12 351–12 359.

Kuroda, K., 2002: Relationship between the polar-night oscillation and the annular mode. *Geophys. Res. Lett.,* **29,** 1240, doi: 10.1029/2001GL013933.

Labitzke, K., 1981: The amplification of height wave 1 in January 1979: A characteristic precondition for the major warming in February. *Mon. Wea. Rev.,* **109,** 983–989.

Limpasuvan, V., and D. L. Hartmann, 1999: Eddies and the annular modes of climate variability. *Geophys. Res. Lett.,* **26,** 3133–3136.

Lorenz, D. J., and D. L. Hartmann, 2003: Eddy–zonal flow feedback in the Northern Hemisphere winter. *J. Climate,* **16,** 1212–1227.

Matsuno, T., 1971: A dynamical model of the stratospheric sudden warmings. *J. Atmos. Sci.,* **28,** 1479–1494.

McIntyre, M. E., 1982: How well do we understand the dynamics of stratospheric warming? *J. Meteor. Soc. Japan,* **60,** 37–64.

North, G. R., T. L. Bell, R. F. Cahalan, and F. J. Moeng, 1982: Sampling errors in the estimation of empirical orthogonal functions. *Mon. Wea. Rev.,* **110,** 699–706.

Norton, W. A., 2003: Sensitivity of Northern Hemisphere surface climate to simulation of the stratospheric polar vortex. *Geophys. Res. Lett.,* **30,** 1627, doi:10.1029/2003GL016958.

O'Neill, A., 1980: The dynamics of stratospheric warmings generated by a general circulation model of the troposphere and stratosphere. *Quart. J. Roy. Meteor. Soc.,* **106,** 659–690.

——, and B. F. Taylor, 1979: Study of the major stratospheric warming of 1976–77. *Quart. J. Roy. Meteor. Soc.,* **105,** 75–92.

——, R. L. Newson, and R. J. Murgatroyd, 1982: An analysis of the large-scale features of the upper troposphere and the stratosphere in a global, three-dimensional, general circulation model. *Quart. J. Roy. Meteor. Soc.,* **108,** 25–53.

Polvani, L. M., and P. J. Kushner, 2002: Tropospheric response to stratospheric perturbations in a relatively simple general circulation model. *Geophys. Res. Lett.,* **29,** 1114, doi:10.1029/2001GL014284.

Quiroz, R. S., 1977: The tropospheric–stratospheric polar vortex breakdown of January 1977. *Geophys. Res. Lett.,* **4,** 151–154.

Robinson, W. A., 2004: Comments on "The structure and composition of the annular modes in an aquaplanet general circulation model." *J. Atmos. Sci.,* **61,** 949–953.

Schoeberl, M. R., 1978: Stratospheric warmings: Observations and theory. *Rev. Geophys. Space Phys.,* **16,** 521–538.

Shindell, D. T., G. A. Schmidt, R. L. Miller, and D. Rind, 2001: Northern Hemisphere winter climate response to greenhouse gas, ozone, solar, and volcanic forcing. *J. Geophys. Res.,* **106** (D7), 7193–7210.

Taguchi, M., 2003: Tropospheric response to stratospheric degradation in a simple global circulation model. *J. Atmos. Sci.,* **60,** 1835–1846.

Thompson, D. W. J., and J. M. Wallace, 1998: The Arctic Oscillation signature in the wintertime geopotential height and temperature fields. *Geophys. Res. Lett.,* **25,** 1297–1300.

——, and ——, 2000: Annular modes in the extratropical circulation. Part I: Month-to-month variability. *J. Climate,* **13,** 1000–1016.

Yoden, S., T. Yamaga, S. Pawson, and U. Langematz, 1999: A composite analysis of the stratospheric sudden warmings simulated in a perpetual January integration of the Berlin TSM GCM. *J. Meteor. Soc. Japan,* **77,** 431–445.

Zhou, S., A. J. Miller, J. Wang, and J. K. Angell, 2002: Downward-propagating temperature anomalies in the preconditioned polar stratosphere. *J. Climate,* **15,** 781–792.